Progress In Electromagnetics Research, Vol. 109, 37–61, 2010

SUPPRESSION OF CROSSTALK USING SERPENTINE GUARD TRACE VIAS

W.-T. Huang

Department of Computer Science and Information Engineering
Minghsin University of Science and Technology
No. 1, Xinxing Road, Xinfeng, Hsinchu 30401, Taiwan, R.O.C.

C.-H. Lu and D.-B. Lin

Graduate Institute of Computer and Communication Engineering
National Taipei University of Technology
No. 1, Section 3, Chung-Hsiao E. Road, Taipei 10608, Taiwan, R.O.C.

Abstract—The reliability of circuits on printed circuit boards (PCBs) in many modern electronic products is affected by severe noise caused by high-speed and low-voltage operation as well as layout constraints compounded by limited space and high circuit density. Crosstalk is a major noise source that interferes with the signal integrity (SI) in poor PCB layout designs. One common method of reducing crosstalk is the three-width (3-W) rule. The serpentine guard trace (SGT) approach has also been used to reduce crosstalk using two terminal matching resistors on the SGT between the aggressor and victim. Although the SGT approach suppresses far-end crosstalk (FEXT) at the expense of more layout space, it also neglects interference caused by near-end crosstalk (NEXT). In this study, we propose the SGT via (SGTV) approach in which grounded vias are added to the SGT at appropriate locations, and the ratio between the lengths of the horizontal and vertical sections of the guard trace is adjusted to minimize NEXT and FEXT. Frequency domain simulated (measured) results showed that the SGTV approach reduced NEXT by 3.7 (7.65) and 0.83 (1.6) dB as well as FEXT by 5.11 (7.22) and 0.1 (1.98) dB compared to the 3-W and SGT approaches, respectively. In the time domain, simulated (measured) results showed that SGTV reduced NEXT by 34.67% (49.8%) and 27.5% (26.65%) as well as FEXT by 46.78% (56.52%) and 6.91% (24.8%) compared to the 3-W and SGT approaches, respectively.

Received 5 September 2010, Accepted 28 September 2010, Scheduled 1 October 2010
Corresponding author: Wen-Tzeng Huang (wthuang@must.edu.tw).

Our proposed approach thus effectively suppresses both NEXT and FEXT to achieve better SI in PCB layout designs than the other two methods. As our design uses two grounded vias instead of two guard trace terminators and does not require extra components, it is less costly than SGT. Our simulated and measured results indicate that our approach is suitable for practical application because of the lower cost and the ease of implementation that eliminates NEXT and FEXT.

1. INTRODUCTION

The progress of modern technology has led to an increasing tendency toward higher speed, greater density, less space, and lower voltages in the design of digital devices and chip packages. These factors increase the difficulty of interconnecting traces and chips on printed circuit boards (PCBs) [1]. The microstrip line structure is the most basic structure of all [2]. Microstrips are widely used in PCB applications and have become the most common forms of interconnection because they are inexpensive and easy to manufacture [3, 4]. As the space between neighboring parallel microstrips is extremely limited in high-density circuit layouts, electromagnetic coupling between them seriously affects signal integrity (SI) by introducing crosstalk [5–10]. Therefore, the ability to avoid crosstalk in PCB layouts is one of the critical factors determining the stability of electronic products. There are two types of crosstalk: near-end crosstalk (NEXT) and far-end crosstalk (FEXT) [11]. These can both be reduced by increasing the spacing between parallel runs, decreasing the thickness of the dielectric, using differential signaling, and minimizing the length of parallel runs. However, all these tradeoffs affect the system cost [12].

The three-width (3-W) rule is a common method of reducing crosstalk [13] in which separation between parallel traces of three times the trace width has been found to reduce the flux boundary by approximately 70% [13]. However, because the remaining 30% flux boundary can still negatively affect the signal quality in high-speed, high-density, space-limited, low-voltage PCB designs, the addition of a guard trace that carries no signal has been proposed to reduce the noise induced in a victim by the aggressor and avoid crosstalk [11, 14–17]. A guard trace that is left unterminated (i.e., open termination) will experience noise and act as a potential source of noise for the victim [11, 17]. Two terminators in the guard trace absorb the noise energy and effectively reduce the crosstalk [17] but increase the cost. Therefore, grounded vias on the guard traces are used instead to reduce crosstalk [18]. A certain number of grounded vias is equivalent to the terminator approach; fewer vias results in more noise, and more vias

perform better than the terminator approach [8].

The pure via approach can reduce crosstalk without requiring extra components [4]. Lee et al. first proposed the serpentine guard trace (SGT) as a means of eliminating FEXT in parallel high-speed interfaces by increasing the capacitive coupling ratio to equal the inductive coupling ratio [3]. The length of the vertical section in the SGT design can increase the mutual capacitance C_m without significantly changing the mutual inductance L_m between the aggressor and victim. Cheng et al. [19] noted that while the grounded guard trace approach is increasingly used to reduce coupling-induced crosstalk, it also introduces ringing that severely limits the performance of microstrip structures. That is, although the increased mutual capacitance can reduce FEXT, this approach results in an increase in NEXT [19]. Moreover, the large number of terminator pairs required in the guard trace increases the cost.

Our SGT via (SGTV) strategy is to combine the use of grounded vias to reduce NEXT and FEXT [19] with the SGT approach to suppress FEXT [3]. We propose a method of calculating the number and location of vias. We also describe a resonance equation in the frequency domain to optimize the resulting performance to reduce NEXT and FEXT across a desired bandwidth. Although our method uses two vias to replace the two terminal matching resistors on the SGT, our approach still results in better signal integrity (SI) of the PCB layout design. Hence, SGTV requires fewer components than the SGT approach [3]. The system cost is lower, the design is simpler, and the result can be implemented more quickly. Simulated and experimental results have clearly demonstrated these advantages of our proposed approach. Our earlier paper discussed "Design of suppressing Crosstalk by Vias of Serpentine Guard Trace" [20].

This paper is organized as follows. Section 2 introduces crosstalk and presents its characteristics. Section 3 discusses SGT characteristics as well as the design methodology and equations for our proposed SGTV approach. Section 4 presents simulated and experimental results that demonstrate how our proposed SGTV effectively suppresses both NEXT and FEXT simultaneously. We present our conclusions in Section 5.

2. CROSSTALK

Crosstalk is the result of the coupling effects caused by C_m and L_m of the victim and aggressor driven by transient signals in the aggressor [21]. Figure 1(a) shows an equivalent model of the two parallel traces and Figure 1(b) shows a typical crosstalk signature of

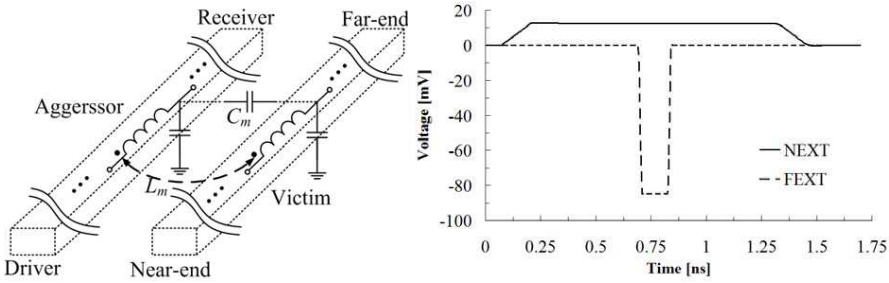

Figure 1. (a) Equivalent model of two parallel traces [1, 3] and (b) typical crosstalk signature of a victim without a guard trace [11, 16].

the victim without a guard trace [11]. The end of the victim closest to the driver (receiver) of the aggressor is referred to as the near (far) end. When the rise and fall times of the aggressor's transient logic states change continually, the signal operation of the victim will be destroyed because the coupling effect of C_m and L_m transfer energy from the aggressor [1]. Crosstalk noise is a major cause of concern in system design because modern high-density circuits have high C_m and L_m values.

For the two parallel traces shown in Figure 1(a), FEXT and NEXT in the victim are the noise voltages induced by the driving and receiving ends of the aggressor, respectively. The FEXT and NEXT waveform in the lossless case can be expressed by Eqs. (1) and (2) [1, 22], respectively, where K_{NE} and K_{FE} are the coefficients of NEXT and FEXT, respectively; they dominate the crosstalk energy. A smaller value of the coefficient indicates less coupling crosstalk noise induced in the victim by the aggressor. Parameters L_S (L_m) and C_S (C_m) are the self (mutual) inductance and self (mutual) capacitance, respectively.

$$K_{NE} = \frac{1}{4} \cdot \left(\frac{C_m}{C_s} + \frac{L_m}{L_s} \right) \tag{1}$$

$$K_{FE} = \frac{1}{2} \left(\frac{C_m}{C_S} - \frac{L_m}{L_S} \right) \tag{2}$$

Our major goal is to obtain smaller values of K_{NE} and K_{FE}. K_{NE} is the sum of the capacitive coupling C_m/C_s and inductive coupling L_m/L_s while K_{FE} is the difference between C_m/C_s and L_m/L_s. However, as L_m/L_s of K_{FE} is greater than C_m/C_s in parallel traces with one side exposed to the air, FEXT is the negative pulse at the rising edge as shown in Figure 1(b).

3. GUARD TRACE

As the seriousness of crosstalk increases with increasing density and speed of circuit layouts, ground traces adjacent to high-speed interconnections are often used to reduce crosstalk in a variety of routing topologies [1, 3] and in high-speed mixed signal systems [4–7]. To suppress crosstalk even further, some studies have proposed using a guard trace, which is one extra trace without any signal between two coupling signal traces [11, 14–17]. As the guard trace acts as a transmission line, it cannot remain at ground potential throughout its entire length [23]. Grounded vias on the guard trace that are connected to the ground plane can enhance the performance of the guard trace, although this will be limited if the number of grounded vias is too small [8].

Via fences, which increase the number of grounded vias on the guard trace, are increasingly used to alleviate crosstalk in dense interconnection layouts because such a fence structure can maintain the ground voltage along the guard trace. Via fences are designed and optimized to reduce coupling noise between two adjacent traces [24]. Although via fences in guard traces show excellent crosstalk reduction performance, this approach requires too many vias in the guard trace to be practical in a PCB layout [3]. An excess of vias renders the PCB structure more fragile to the point where the PCB may not support some components securely [25]. Huang et al. first proposed a method of calculating the optimal number of grounded vias required to prevent crosstalk and obtain maximum efficiency. The appropriate guard trace segment distance calculated with this method will change the position of a pulse in the victim so that a negative pulse offsets a positive pulse to reduce crosstalk [25]. This paper presents a technique based on an additional trace grounded by vias with which the crosstalk can be reduced by 50%–90% [18]. SPICE circuit analysis software was used to analyze a lumped circuit T-structure model of three coupled lines. The via discontinuities were modeled in a novel way to account for their transient skin effect resistance. Multimodal analysis of guard traces was also performed [26] using a model that allows rigorous and quantitative analysis of guard trace configurations. Ladd and Costache first used the "two-dimensional finite element method" to compute the distributed capacitance and inductance parameters of the coupled printed circuit tracks in 1992 [18]. This strategy of using guard trace vias reduces C_m and L_m together, and can therefore simultaneously reduce NEXT and FEXT [18, 19].

3.1. Serpentine Guard Trace

Interference in electronic products increases with increasing speed and density and with decreasing operating voltage and circuit size. Lee et al. [3] proposed the SGT with the structure shown in Figure 2(b) as a guard trace for reducing interference [3]. This SGT structure consists of horizontal and vertical guard trace sections. The horizontal section is near both the victim and aggressor to increase C_m. As the vertical section of the guard trace is perpendicular to the victim and aggressor, it will not increase electromagnetic coupling. Table 1 shows the parameters L_S, L_m, C_S, and C_m measured using an LCR

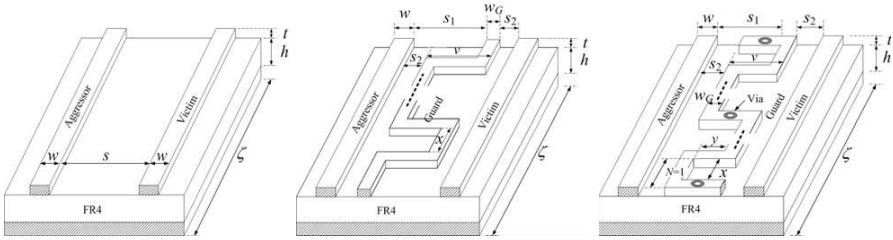

Figure 2. Comparison of three topologies: (a) 3-W rule [13], (b) SGT [3], and (c) SGTV.

Table 1. Parameters L_S, L_m, C_S, and C_m measured using an LCR meter [3].

	3-W [13]	Conv. guard [8]	Via guard [8]	SGT [3]	
L_S [nH/m]	456	456	452	456	
L_m [nH/m]	16.8	16.7	7.84	16.0	
C_S [pF/m]	119	122	121	125	
C_m [pF/m]	0.90	1.90	0.40	3.10	
K_{NE}	0.011101	0.013049	0.000516	0.014972	Note 1
K_{FE}	−0.01464	−0.01052	−0.00702	−0.00514	Note 2

Note 1: K_{NE} is our extra computing result according to Eq. (1).
Note 2: K_{FE} is the original result [3].

meter [3], as well as K_{NE} and K_{FE} [3, 8, 13]. As this SGT design can increase C_m up to 3.10 pf/m in Table 1 without increasing L_m [3], $K_{FE} = -0.00514$ of the SGT is the lowest in Table 1; the SGT design thus reduces FEXT. The terminal resistors on both SGT terminals to match its characteristic resistance absorb the coupled energy of the signal. Therefore, the SGT design effectively reduces the second coupling effect and provides stable protection capability [3].

Although SGT can effectively reduce FEXT, it has two disadvantages. First, while SGT reduces K_{FE}, this design increases $K_{NE} = 0.0149172$ in Table 1 [19]. A design with many parallel high-speed interfaces would require a large number of resistors to suppress crosstalk [4] and would thus cost more. Therefore, we propose a new SGTV design in which grounded vias are added to the SGT as shown in Figure 2(c). Our proposed methodology can overcome the two disadvantages of the SGT approach.

3.2. Serpentine Guard Trace Vias

Moreover, Mbairi et al. proposed the performance concept of the guard trace with grounded vias that electrical field lines can be early conducted to ground by vias of guard trace and magnetic field lines will be isolated by the guard trace with grounded vias for alleviating the interference from the aggressor by HFSS in 2007 [27]. Simultaneously, the current on the guard trace can be quickly conducted to ground by vias. Hence, both electrical and magnetic fields can be reduced their interference effect from the aggressor to victim such that both C_m and L_m can be effectively reduced in the guard trace with grounded vias structure [19], while the SGT can increase C_m [3]. Our proposed topology, the structure of which is shown in Figure 2(c), combines the advantages of these two approaches. As our method uses two vias to replace the two terminal matching resistances in the SGT approach, SGTV requires fewer components [3] and will lend itself to widespread use in practical applications.

Although the SGTV approach is an incremental improvement of SGT using grounded vias, the metric units for layout size in [3] will be changed to Imperial units for implementation reasons because we wish to collect measured results for the topologies shown in Figure 2 and verify that our approach can simultaneously reduce both of FEXT and NEXT. All the measurement parameters of these topologies are the same as in [3]. We chose our parameter values as follows in accordance with Figure 2(c): PCB material, FR4 with dielectric constant $\tan(\delta) = 0.035$; PCB thickness = 7 mil, copper thickness = 1.4 mil, width of both aggressor and victim = 12 mil, guard trace width w_G = 6 mil, space between aggressor and victim = 36 mil, space between guard

trace and aggressor $s_1 = 24\,\text{mil}$, space between guard trace and victim $s_2 = 6\,\text{mil}$, total trace length $= 4000\,\text{mil}$, horizontal section length of guard trace $x = 50\,\text{mil}$, vertical section length of guard trace $v = 24\,\text{mil}$, characteristic impendence of aggressor and victim $= 50\,\Omega$, and characteristic impendence of guard trace $= 68\,\Omega$. The IE3D simulation tool [28] was used to obtain the capacitance and inductance parameters at 60 MHz. Table 2 shows the simulation results for various parameters for the three models: 3-W [13], SGT [3], and SGTV. Our results showed that the SGTV values of K_{NE} and K_{FE} were less than 36.4% and 40.6% of the corresponding 3-W values. Moreover, the SGTV values of K_{NE} and K_{FE} were less than 43.1% and 37.1% of the corresponding SGT values. SGTV can thus reduce both K_{NE} and K_{FE}.

The two terminal resistors added to the SGT terminals to match its characteristic resistance absorb the coupled signal energy [3]. As grounded vias in the SGTV design are used to absorb the noise energy instead of the terminal resistors used in the SGT design, the cost is lower because there are fewer components. Therefore, a large number of SGTV grounded vias can be used. The major reason for using vertical and horizontal sections in [1] was to increase C_m. As described above, such mutual capacitance decreases both FEXT and K_{FE}, as shown in Eq. (2), while increasing both NEXT and K_{NE}, as shown in Eq. (1). Table 2 compares the K_{FE} and K_{NE} values for the 3-W [13], SGT [3], and SGTV approaches. As the SGTV values of $C_m = 0.384\,\text{pF/m}$ and $L_m = 5.148\,\text{nH/m}$ are the lowest in the whole table, the SGTV values of $K_{FE} = -0.005925$ and $K_{NE} = 0.004632$ are also the lowest. Four of the SGTV parameters are indicated as being "Reduced" in Table 2. Therefore, combining grounded vias in the guard trace and adjustment of the vertical and horizontal section ratio and dimensions can simultaneously reduce FEXT and NEXT.

Table 2. Simulation results for three models with various extracted parameters.

	3-W [13]	SGT [3]	SGTV	SGTV advantages
L_S (nH/m)	342.26	342.25	338.96	
L_m (nH/m)	8.552	8.555	5.148	Reduced
C_S (pF/m)	114.25	114.29	114.94	
C_m (pF/m)	0.475	0.705	0.384	Reduced
K_{NE}	0.007286	0.00791	0.004632	Reduced
K_{FE}	−0.010415	−0.009413	−0.005925	Reduced

3.3. Serpentine Guard Trace Design

In SGT design, the ratio between the vertical and horizontal sections can increase C_m without changing the other three parameters C_s, L_m, and L_s [3]. The SGT reduces the difference between the capacitance and inductance couplings resulting in a smaller K_{FE} and hence lower FEXT at the expense of greater NEXT and larger K_{NE} coefficient [19]. Our proposed design concept is to adjust the ratio between the vertical and horizontal sections to decrease C_m and L_m simultaneously as shown in Table 2. Smaller values of C_m and L_m lead to smaller K_{FE} and K_{NE} coefficients, respectively. Therefore, our proposed SGTV design can effectively reduce both FEXT and NEXT at the same time.

For verification, the total length of the transmission lines was first fixed at 4000 mil while the dimensions and ratio of the vertical and horizontal sections were determined later. The parameters C_m, C_s, L_m, and L_s of the three models were substituted into Eqs. (1) and (2) to help in determining a better ratio between the vertical and horizontal section sizes. The vertical SGTV section was fixed, while the length of the horizontal section was gradually increased to analyze its effect and illustrate our design concept. The length and width of both the aggressor and victim were set to 4000 and 12 mil, respectively. Figure 3 shows a bird's-eye view of the 4000-mil total length. The width of the SGT was set to 6 mil. The length of the horizontal section was $x = 50$ mil and the length of the vertical section was $v = 24$ mil. Both the transmission and guard traces were 1.4 mil thick, the thickness of the FR4 PCB was 7 mil, the dielectric constant of FR4 was 0.035, and the space between two neighboring traces was 6 mil. These parameters determine the characteristic impedance of both the victim and aggressor (50 Ω) and the characteristics impedance of the SGT (68 Ω).

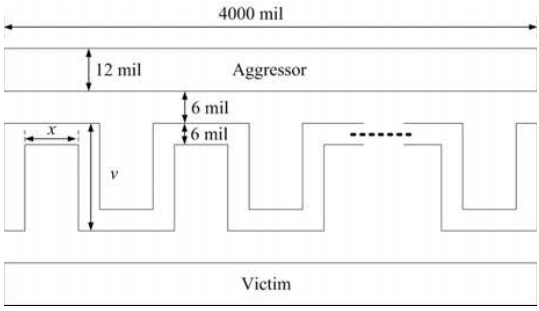

Figure 3. Bird's-eye view of 4000-mil total length.

To determine the average performance in reducing NEXT and FEXT, an index $(K_{NE} + |K_{FE}|)/2$ is used to evaluate the effects of both K_{NE} and K_{FE}. The use of $|K_{FE}|$ is simply for convenience to ensure the index remains positive. A lower value of index $(K_{NE} + |K_{FE}|)/2$ indicates lower values of both NEXT and FEXT, i.e., better performance. The value of $(K_{NE} + |K_{FE}|)/2$ can be displayed for a simulated horizontal section length in the range of 60–2000 mil, while all parameters are extracted by the simulation tool for a frequency of 60 MHz. Figure 4(a) shows the relationship between the length of the horizontal section and the performance index $(K_{NE} + |K_{FE}|)/2$. Figure 4(b) shows an expanded view of 4(a) for the region about 500 mil horizontal section length. In Figure 4(b), $(K_{NE} + |K_{FE}|)/2 = 0.008662$ is the minimum for a horizontal section length of 120 mil. As the total length of the trace for the simulation was set at 4000 mil, horizontal section lengths greater than 2000 mil are not discussed here because this would result in an asymmetric SGTV length and non-uniform

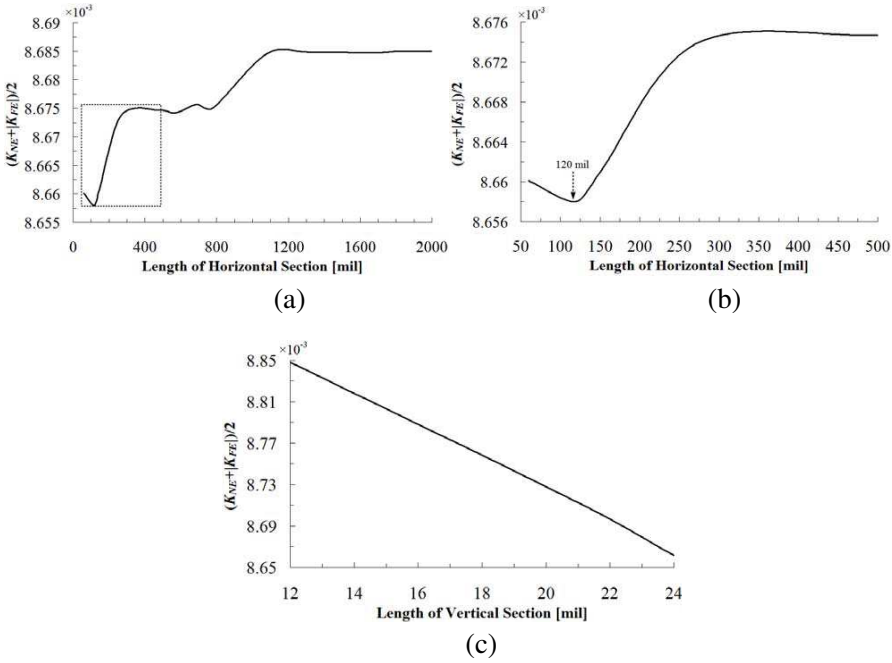

Figure 4. Effects of SGTV dimensions on the performance index $(K_{NE} + |K_{FE}|)/2$: (a) horizontal section length, (b) expanded view of (a) showing the region about 500 mil horizontal section length, and (c) vertical section length.

performance. The next step is to obtain a better structure for simultaneously reducing both NEXT and FEXT.

Simulations were conducted for horizontal sections lengths of 90, 120, 270, and 480 mil because they were easy to implement on the PCB. All available parameters in the structure can be extracted by the simulation tool [23] at 60 MHz [3, 11]. Table 3 shows the parameters C_m, C_s, L_m, L_s, K_{NE}, K_{FE}, and $(K_{NE}+|K_{FE}|)/2$ for the four different horizontal section lengths and a total length of 4000 mil.

Similar to the method used for the horizontal cases, the range of the simulated vertical section was 12–24 mil. Figure 4(c) shows the relationship between the vertical length and performance index $(K_{NE} + |K_{FE}|)/2$. Our design will not consider the case where the length of the vertical section is narrower than 12 mil because this would be an irregular design; the width of the guard trace, aggressor, and victim are all 12 mil. Moreover, our study does not consider the case where the length of the vertical section is wider than 12 mil because this would be difficult to implement practically on the PCB. The lengths of the vertical section used in the simulation were representative values of 12, 21, and 24 mil. Parameters C_m, C_s, L_m, and L_s, can be extracted by the simulation tool at 60 MHz. Table 4 shows these parameters as well as K_{NE}, K_{FE}, and $(K_{NE} + |K_{FE}|)/2$ for the three different vertical section lengths with horizontal section lengths less than 120 mil and a total length of 4000 mil. This table clearly shows that longer vertical section lengths give better performance because higher values of C_m result in lower values of K_{FE} and lower FEXT. For example, $C_m = 0.6005$ pF/m for $v = 21$ mil is greater than $C_m = 0.4883$ pF/m for $v = 12$ mil, and thus $K_{FE} = -0.009864$ for 21 mil is less than $K_{FE} = -0.010373$ for 12 mil.

The length of the horizontal section affects C_m and influences the crosstalk in SGTV. First, the coupling length was varied from 2000

Table 3. Parameters for the four different horizontal section lengths.

	$x = 90$ mil	$x = 120$ mil	$x = 270$ mil	$x = 480$ mil
L_S (nH/m)	342.23	341.99	342.24	342.04
L_m (nH/m)	8.6147	8.6017	8.6157	8.6098
C_S (pF/m)	114.26	114.26	114.25	114.24
C_m (pF/m)	0.7081	0.7037	0.7007	0.6988
K_{NE}	0.007842	0.007828	0.007827	0.007822
K_{FE}	−0.009488	−0.009496	−0.009521	−0.009527
$(K_{NE}+\|K_{FE}\|)/2$	0.008665	0.008662	0.008674	0.008675

Table 4. Parameters for three vertical section lengths, a horizontal section length of 120 mil, and a total length of 4000 mil.

	$v = 12$ mil	$v = 21$ mil	$v = 24$ mil
L_S (nH/m)	342.27	341.49	341.99
L_m (nH/m)	8.5633	8.5322	8.6017
C_S (pF/m)	114.25	114.22	114.26
C_m (pF/m)	0.4883	0.6005	0.7037
K_{NE}	0.007323	0.007561	0.007828
K_{FE}	−0.010373	−0.009864	−0.009496
$(K_{NE} + \|K_{FE}\|)/2$	0.008848	0.008712	0.008662

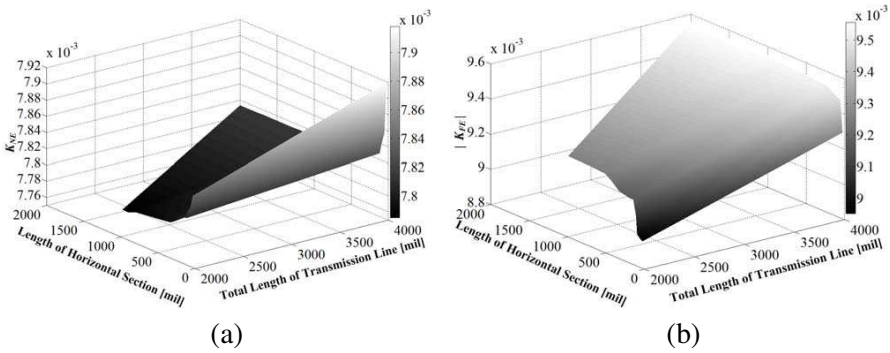

(a) (b)

Figure 5. Relationship among the crosstalk coefficient, horizontal section length, and total length of the transmission line for (a) K_{NE} and (b) $|K_{FE}|$.

to 4000 mil and the horizontal section length was varied from 0 to 2000 mil in the simulation. Figure 5(a) shows the interrelationship of the horizontal section length of the guard trace, the total trace length, and K_{NE}. The results indicate a direct relationship between the total trace length and K_{NE}, and an inverse relationship between the horizontal section length and K_{NE}. That is, a longer transmission trace results in a higher value of K_{NE} because it increases L_m/L_s, and a longer horizontal section results in a lower value of K_{NE} because the decreased ratio C_m/C_s is less than the increased ratio of L_m/L_s.

Figure 5(b) shows the interrelationship of the horizontal section length of the guard trace, the total length of the trace, and $|K_{FE}|$, the last of which is plotted on the z-axis. The results indicate that both the total length of the trace and the horizontal section length

are directly proportion to $|K_{FE}|$. That is, a longer transmission trace results in a higher value of $|K_{FE}|$ due to the increase in L_m/L_s and the decrease in C_m/C_s.

Therefore, a longer total trace length will cause more NEXT and FEXT because its coupling segment is longer. Increasing the horizontal section length of the SGT reduces K_{NE} and increases K_{FE}. Based on the discussion above, the results show that one design will increase C_m and reduce FEXT at the expense of increased NEXT. However, using our approach, we can adjust the horizontal section length of the SGT to reduce K_{NE} and K_{FE} simultaneously. Better selection of the horizontal length will result in better overall performance by reducing both NEXT and FEXT. Figure 6(a) shows the effects of Nor[Nor(K_{NE}) + |Nor(K_{FE})|] on NEXT and FEXT, were Nor() is the normalization function. This normalization function can obviously represent the relative crosstalk ratio of NEXT and FEXT.

Obtaining better performance by adjusting the ratio between horizontal section length and total transmission line length requires a two-step operation. The first step is to normalize the results of Figures 5(a) and (b), and the second is to add the two results of the first step. Hence, the guard trace results indicate better performance of the valley line, for horizontal section lengths of 120–128 mil and total transmission line lengths of 2000–4000 mil for reducing crosstalk. Therefore, the segment valley is redrawn as shown in Figure 6(b). The results shown in Table 4 indicate that a longer vertical section causes more NEXT and less FEXT. Therefore, the vertical section of SGTV is as long as possible because a higher value of C_m will produce a higher value of K_{FE} and less FEXT. Finally, the space between the aggressor

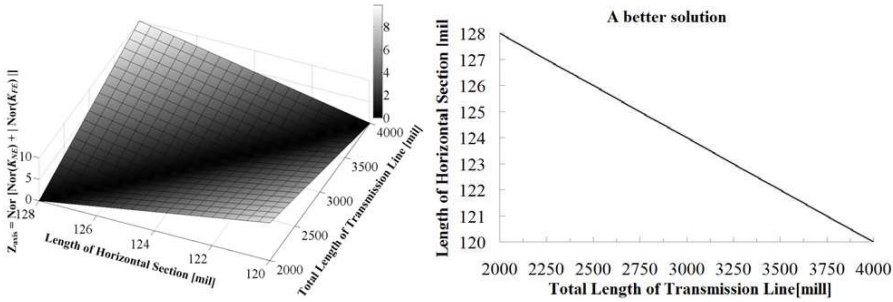

Figure 6. Total effect on FEXT and NEXT including (a) three-dimensional sketch, and (b) optimum ratio of the horizontal section length and the total transmission line length.

and victim is three times the trace width. Under this limitation, the vertical section of SGTV is as long as possible. Figure 6(b) shows the optimum ratio of the total length of the trace (x-axis) to the SGTV horizontal section length (y-axis) as a straight line.

3.4. Results After Adjusting Parameters

The dimensions of all guard traces were adjusted to $x = 120\,\text{mil}$ and $v = 24\,\text{mil}$ with two terminating resistors on the SGT. The simulation tool [28] was used to obtain the capacitance and inductance parameters for 60 MHz as shown in Table 5. The $\text{SGTV}_{\text{after}}$ column indicates values after adjusting the length of the horizontal section so that C_m increased slightly from 0.384 pF/m to 0.391 pF/m and L_m decreased slightly from 5.148 nH/m to 4.833 nH/m. The SGTV structure is the same as SGT [3], and $\text{SGTV}_{\text{after}}$, which will be discussed later, is a variation of SGTV. Hence, compared to the SGTV design, $\text{SGTV}_{\text{after}}$ gives 4.6% better performance based on K_{NE} and 8.2% better performance based on K_{FE}. Therefore, adjusting the length proportion of the horizontal section can effectively reduce both the NEXT and FEXT of the SGTV approach. The grounded vias were used in the SGTV approach to absorb the noise energy and effectively reduce the crosstalk without requiring two matching resistors. Resonance will occur in the frequency domain [18] because of the vias on the SGTV. To obtain the relationship between resonance and the SGTV bandwidth, the resonance is calculated as described in the next section.

3.5. Resonance of the Serpentine Guard Trace Vias

This section discusses our proposed equations. First, to adjust the distance between two neighboring vias to control the location of the resonance [24, 29], a small number of vias are added to the SGTV

Table 5. Parameters from the simulation results.

	3-W [13]	SGT [3]	SGTV	$\text{SGTV}_{\text{after}}$
L_S(nH/m)	342.26	342.25	338.96	338.49
L_m (nH/m)	8.552	8.555	5.148	4.833
C_S (pF/m)	114.25	114.29	114.94	114.93
C_m (pF/m)	0.475	0.705	0.384	0.391
K_{NE}	0.007286	0.007792	0.004632	0.004419
K_{FE}	−0.010415	−0.009413	−0.005925	−0.005439

structure. The relationship between the number of vias and the number of the serpentine amount is investigated later. We will discuss our proposed equation in detail.

To facilitate the explanation of the SGTV resonance, some related parameters in Figure 2(c) are substituted and rearranged to give the SGTV structure shown in Figure 7. The total length ζ (width of w) of the aggressor and victim is 4000 (12) mil. Let w_G, x, v, and y be the SGTV width (6 mil), the length of the horizontal section (120 mil), the length of the vertical section (24 mil), and the vertical distance (12 mil), respectively. In addition, N is the number of the serpentine amount, t is the thickness of both the trace and the SGT (1.4 mil), h is the PCB thickness (7 mil), ε_r be is dielectric coefficient of FR4 (4.664), $\tan\delta$ is the dielectric loss (0.035), s_1 is the space between guard trace and aggressor (24 mil), and s_2 is the space between the guard trace and victim (6 mil). In addition, the via diameter is 9 mil. The parameters of this design determine the characteristic impendence of both the aggressor and the victim as 50 Ω and the characteristic impendence of SGTV as 68 Ω. Thus, the relationship between y and v is given by

$$v{=}y{+}2w \tag{3}$$

The resonance phenomenon caused by the vias on the SGT has been discussed previously [10, 29]. Hence, the equation in [29] can be rewritten as Eq. (4) where f, K, L, and ε_{reff} are the resonance frequency, the number of resonances, the distance between two neighboring vias, and the dielectric coefficient of the microstrip line, respectively.

$$f{=}K \cdot \frac{3 \times 10^8}{2L\sqrt{\varepsilon_{reff}}} \quad K = 1, 2, 3, \ldots \tag{4}$$

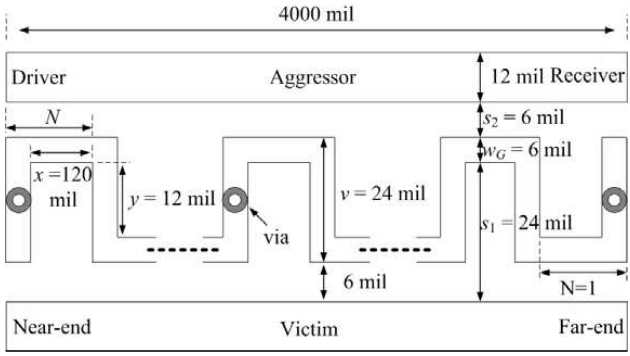

Figure 7. SGTV configuration.

Equation (4) shows that the distance between two neighboring vias will affect the resonance location. Hence, adjusting the location of the vias will control the resonance. In addition, because the current in the serpentine guard induced by the aggressor will be changed by the bent sections (called Γ-junctions) of the SGT at high frequencies, the induced current, which is concentrated on the inner side of the bent sections, of the following distance on the SGT will be changed [30]. Hence, our proposed Eq. (5) revises the following current of the equivalent distance at the bent section. Then, substituting the relationship between the vias and number of the serpentine amount, the resonance order position can be adjusted by controlling the number of the serpentine amount. Let L be the distance between two neighboring vias on the microstrip line, and N be the number of the serpentine amount as before. In addition, let x, y, and w be the SGTV horizontal length, vertical distance, and the width, respectively.

$$L = N \times (x+y+w) \tag{5}$$

Based on the results reported previously [31], obtaining the dielectric coefficient for the microstrip structure requires another calculation. Eq. (6) shows the equation for calculating ε_{reff} where F is the correction coefficient from Eq. (7), h is the PCB thickness, w is the trace width, and t is the trace thickness.

$$\varepsilon_{reff} = \frac{\varepsilon_r+1}{2} + \frac{\varepsilon_r-1}{2}\left(1+\frac{12h}{w}\right)^{-1/2} + F - 0.217\,(\varepsilon_r-1)\,\frac{t}{\sqrt{wh}} \tag{6}$$

$$F = \begin{cases} 0.02\,(\varepsilon_r-1)\left(1-\frac{w}{h}\right)^2 & \text{for } \frac{w}{h} < 1 \\ 0 & \text{for } \frac{w}{h} > 1 \end{cases} \tag{7}$$

To simplify the explanation of Eqs. (4)–(7), let $\mathrm{SGTV_{3N}}$ ($\mathrm{SGTV_{4N}}$, $\mathrm{SGTV_{5N}}$, $\mathrm{SGTV_{6N}}$) indicate the configuration in which two neighboring vias are located between 3 (4, 5, 6) serpentines in the SGTV. The parameters shown in Figure 7 are used here. When the parameters of the $\mathrm{SGTV_{5N}}$ structure, with two vias located between five serpentines, are substituted into Eqs. (4)–(7), the resonance frequency occurs at 4.73 GHz. The simulation results using the simulation tool [28] were used to verify that the proposed equations were correct. Our simulation results presented in Figure 8(a) agreed with the calculated value for the first resonance frequency in $\mathrm{SGTV_{5N}}$ indicating that our proposed equations are correct. The NEXT and FEXT of the simulated results for $\mathrm{SGTV_{3N}}$, $\mathrm{SGTV_{4N}}$, $\mathrm{SGTV_{5N}}$, and $\mathrm{SGTV_{6N}}$, referred to as $\mathrm{SGTV_{after}}$, are shown in Figures 8(a) and 8(b), respectively, in the frequency domain. Therefore, designers can use our methodology to select the number of vias to meet the bandwidth requirement to achieve optimum SGTV performance.

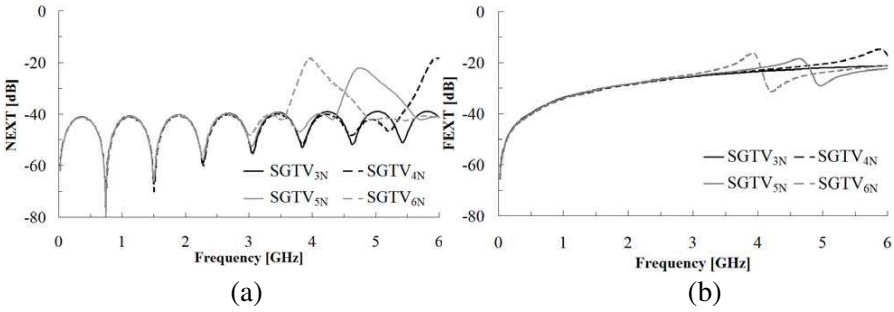

Figure 8. Frequency response of the SGTV design with different numbers of vias for (a) NEXT and (b) FEXT.

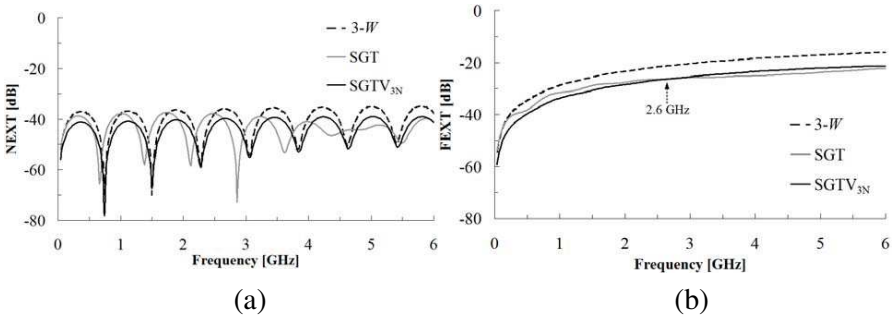

Figure 9. Simulated results of (a) NEXT and (b) FEXT.

4. SIMULATED AND MEASURED RESULTS

Figures 2(a), 2(b), and 2(c) show the simulated and experimental results in the frequency and time domains for the 3-W, SGT, and SGTV structures, respectively. We wish to verify that the SGTV FEXT and NEXT values are the lowest. Our SGTV structure can suppress crosstalk up to 6 GHz, because there is no resonance in the $SGTV_{3N}$ structure during 6 GHz. Table 6 shows all parameters used and our verified results.

4.1. Simulated Results

Figures 9(a) and 9(b) show the simulated frequency domain NEXT and FEXT [28] of the three approaches.

The operating frequency of most modern electronic products is less than 6 GHz [32]. Therefore, our SGTV design concept focuses on frequencies below 6 GHz. An intersection point was observed for FEXT

Table 6. Parameter listing for simulation and experiment.

Parameter	without guard trace	with serpentine guard trace	
	3-W[13]	SGT [3]	$\text{SGTV}_{3\text{N}}$
ε_r	4.664		
Loss tangent (δ)	0.35		
h (mil)	7		
t (mil)	1.4		
w (mil)	12		
w_G (mil)	NA (Note3)	6	
s (mil)	36		
s_1 (mil)	NA	24	
s_2 (mil)	NA	6	
x	NA	50	120
v	NA	24	
y	NA	12	
ζ (mil)	4000		
(Aggressor and Victim) Z_O (Ω)	50		
(SGT) Z_O (Ω)	68		

Note 3: NA, not applicable [27].

Table 7. Average performance according to the simulation results for the frequency and time domains.

	Frequency-domain		Time-domain	
	NEXT (dB)	FEXT (dB)	NEXT peak (mV)	FEXT peak (mV)
3-W	−40.84	−22.85	15.66	−106.78
SGT	−43.71	−27.86	14.11	−61.05
$\text{VSGT}_{3\text{N}}$	−44.54	−27.96	10.23	−56.83

in Figure 9(b). As selecting the better design is difficult simply using curves, we added all decibel values below 6 GHz and then averaged them as shown in Table 7.

Table 7 shows the averages of the simulation results in the frequency domain for the 3-W, SGT, and $\text{SGTV}_{3\text{N}}$ approaches.

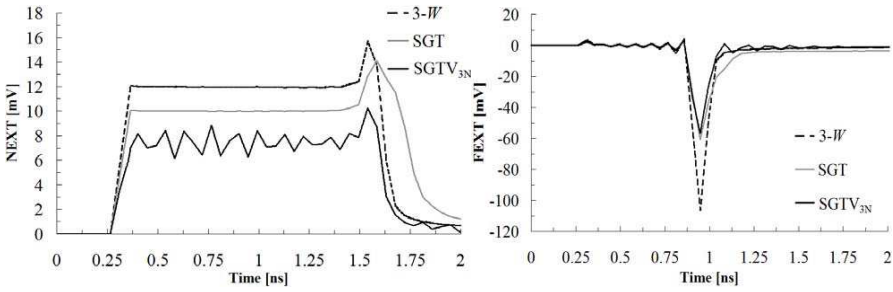

(a) (b)

Figure 10. Simulation performance in the time domain of (a) NEXT and (b) FEXT.

Compared to the 3-W results, our proposed SGTV showed better performance by about 3.7 dB for NEXT and 5.11 dB for FEXT in the frequency domain. Compared to the SGT structure, SGTV performed better by about 0.83 dB for NEXT and 0.1 dB for FEXT in the frequency domain. Hence, our proposed structure had outperformance of the three in the frequency domain for both NEXT and FEXT.

Next, we examined the performance in the time domain. Let the rise time and amplitude of the input step signal be 100 ps and 3.3 V, respectively. Figures 10(a) and (b) show the simulation results for NEXT and FEXT, respectively, in the time domain for the 3-W, SGT, and $SGTV_{3N}$, approaches, and Table 7 shows the peak values. The NEXT evaluated by its peak was 15.66, 14.11, and 10.23 mV for 3-W, SGT, and $SGTV_{3N}$, respectively. The FEXT of 3-W, SGT, and $SGTV_{3N}$ was -106.78, -61.05, and -56.83 mV, respectively. These observations show that in the time domain, the SGTV approach can reduce NEXT by 34.67% and 27.5% more than of 3-W and SGT, respectively, and reduce FEXT by 46.78% and 6.91% more than 3-W and SGT, respectively. Thus, our proposed methodology clearly showed outperformance of the three.

4.2. Experimental Results

Figure 11 shows the physical prototypes of the 3-W, SGT, and $SGTV_{3N}$ topologies constructed with the same parameters used in the simulations (Table 6 and Figure 2) to test their experimental performance. Crosstalk in the victim was measured using an Agilent E8362B network analyzer in the frequency domain [29]. Figures 12(a) and 12(b) show the measured NEXT and FEXT results.

Figure 12 shows that the NEXT and FEXT performance of the SGTV is outperformance of the three approaches. Table 8 shows the frequency domain average.

Table 8 shows that our $SGTV_{3N}$ approach can improve NEXT by 7.65 dB compared to the 3-W approach and 1.6 dB compared to the SGT approach in the frequency domain. For FEXT, the equivalent figures were 7.22 and 1.98 dB. Our structure thus has outperformance of the three.

We used the same input signal for the time domain experiments that was used in the simulation: i.e., step signal of 3.3 V with a rise time of 100 ps. Figures 13(a) and 13(b) show the experimental results

Table 8. Average experimental performance in the frequency and time domains.

	Frequency-domain		Time-domain	
	NEXT (dB)	FEXT (dB)	NEXT peak (mV)	FEXT peak (mV)
3-W	−25.59	−22.52	49.9	−100.64
SGT	−31.64	−27.76	34.15	−58.19
$VSGT_{3N}$	−33.24	−29.74	25.05	−43.76

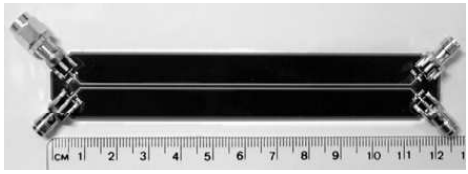

(a)

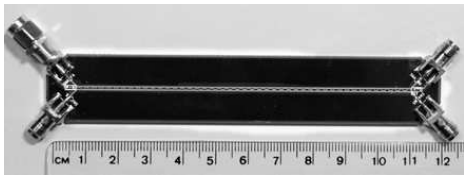

(b)

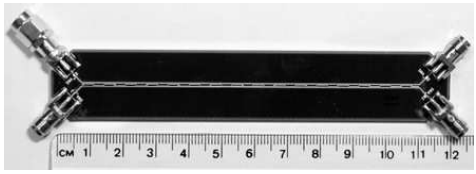

(c)

Figure 11. Photographs of the physical prototypes of (a) 3-W, (b) SGT, and (c) SGTV topologies.

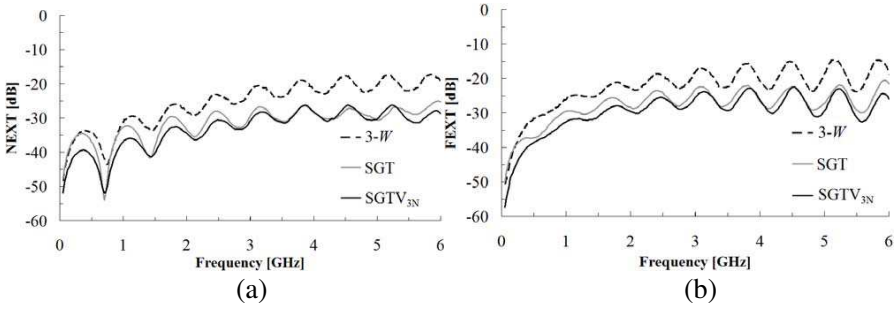

Figure 12. Experimental results in the frequency domain for (a) NEXT and (b) FEXT.

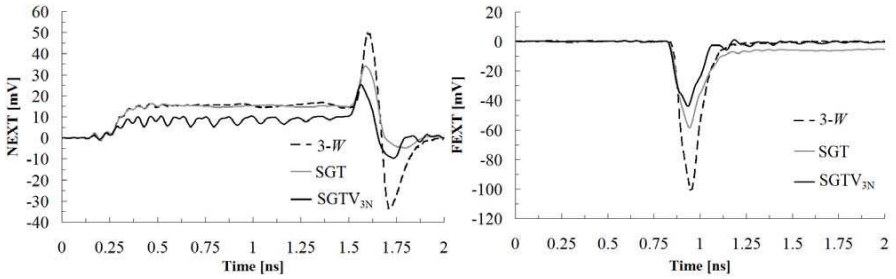

Figure 13. Experimental results in the time domain for (a) NEXT and (b) FEXT.

for NEXT and FEXT, while Table 8 shows the peak values. In the time domain, SGTV reduced the NEXT by 49.8% compared to the 3-W approach and by 26.6% compared to the SGT approach. For FEXT, the equivalent values were 56.6% and 24.8%, respectively. Thus, our approach has outperformance of the three in the time domain as well as in the frequency domain.

There were small differences between the simulated and experimental results for several reasons. First, while the tested PCB trace was originally set to 50 Ω, this changes slightly during crosstalk that simultaneously excites the odd and even modes [33]. In addition, connection loss occurs between the connector and the PCB [25]. Hence, there is a slight difference about the 50-Ω impedance characteristic between the simulated and experimental cases. These errors aside, our simulation and experimental results both indicated that the performance of our proposed SGTV was indeed better than those of 3-W and SGT topologies for suppressing both NEXT and FEXT.

5. CONCLUSION

We have proposed the SGTV structure, which uses grounded vias on the SGT to provide effective suppression of both NEXT and FEXT simultaneously. Unlike the SGT approach, which requires extra components on the guard trace and can suppress only FEXT, our design uses vias and suppresses both NEXT and FEXT. We have proposed a design rule to determine the total length and the horizontal section length of the trace to achieve optimum performance. In addition, we developed a method for determining the number and spacing of vias to achieve the desired bandwidth. Together, these can be used to quickly create the SGTV structure. The simulated and experimental results showed good agreement, and demonstrated that our SGTV design is valid. In the frequency domain, the simulated (measured) results indicated that SGTV could improve NEXT by 3.7 (7.65) dB compared to the 3-W approach and 0.83 (1.6) dB compared to the SGT approach. The equivalent figures for FEXT were 5.11 (7.22) and 0.1 (1.98) dB, respectively. In the time domain, the simulated (measured) results indicated that SGTV improved NEXT by 34.67% (49.8%) compared to the 3-W approach and 27.5% (26.65%) compared to the SGT approach. The equivalent figures for FEXT were 46.78% (56.52%) and 6.91% (24.8%) dB, respectively.

These simulated and experimental results confirmed that our proposed SGTV structure not only shows better performance than the alternatives, but also requires no extra components such as terminating resistors to reduce noise significantly. The suppression of NEXT and FEXT is quite effective and our design may be used in practical engineering solutions.

ACKNOWLEDGMENT

The authors would like to thank the National Science Council of the Republic of China for financially supporting this research under Contract 98-2622-E-159-003-CC3 and NSC 98-2221-E-166-008-.

REFERENCES

1. Sharawi, M. S., "Practical issues in high speed PCB design," *IEEE Potentials*, Vol. 23, No. 2, 24–27, Apr.–May 2004.
2. Kim, J., H. Lee, and J. Kim, "Effects on signal integrity and radiated emission by split reference plane on high-speed multilayer printed circuit boards," *IEEE Transactions on Advanced Packaging*, Vol. 28, No. 4, 724–735, Nov. 2005.

3. Lee, K., H. B. Lee, H. K. Jung, J. Y. Sim, and H. J. Park, "A serpentine guard trace to reduce the far-end crosstalk voltage and the crosstalk induced timing jitter of parallel microstrip lines," *IEEE Transactions on Advanced Packaging*, Vol. 31, No. 4, 809–817, Nov. 2008.
4. Lee, K., H. K. Jung, H. J. Chi, H. J. Kwon, J. Y. Sim, and H. J. Park, "Serpentine microstrip line with zero far-end crosstalk for parallel high-speed DRAM interfaces," *IEEE Transactions on Advanced Packaging*, Vol. 33, No. 2, 552–558, May 2010.
5. Jarvis, B. D., "The effects of interconnections on high-speed logic circuits," *IEEE Transactions on Electronic Computers*, Vol. 12, No. 5, 476–487, Oct. 1963.
6. Feller, A., H. R. Kaupp, and J. J. Digiacomo, "Crosstalk and reflections in high-speed digital systems," *Fall Joint Computer Conference*, 511–525, Las Vegas, NV, Nov. 1965.
7. Sohn, Y. S., J. C. Lee, H. J. Park, and S. I. Cho, "Empirical equations on electrical parameters of coupled microstrip lines for crosstalk estimation in printed circuit board," *IEEE Transactions on Advanced Packaging*, Vol. 24, No. 4, 521–527, Nov. 2001.
8. Chen, H. and Y. Zhang, "A synthetic design of eliminating crosstalk within MTLS," *Progress In Electromagnetics Research*, Vol. 76, 211–221, 2007.
9. Xiao, F., R. Hashimoto, K. Murano, and Y. Kami, "Analysis of crosstalk between single-ended and differential lines," *PIERS Online*, Vol. 3, No. 1, 2007.
10. Kayama, S., M. Sonehara, T. Sato, K. Yamasawa, and Y. Miura, "Cross-talk suppression in high-density printed circuit boards using magnetic composite filled in spacing between signal lines," *IEEE Transactions on Magnetics*, Vol. 45, No. 10, 4801–4803, Oct. 2009.
11. Bogatin, E., *Signal Integrity-simplified*, Prentice Hall, 2003.
12. Hall, S. H. and H. L. Heck, *Advanced Signal Integrity for High-speed Digital System Design*, Wiley, Hoboken, NJ, 2009.
13. Montrose, M. I., *EMC and the Printed Circuit Board: Design, Theory, and Layout Made Simple*, IEEE Press, 1998.
14. Chilo, J. and T. Arnaud, "Coupling effects in the time domain for an interconnecting bus in high-speed GaAs logic circuits," *IEEE Transactions Electron Devices*, Vol. 32, No. 3, 347–352, Mar. 1984.
15. You, H. and M. Soma, "Crosstalk analysis of interconnection lines and packages in high-speed integrated circuits," *IEEE Transactions on Circuits and Systems*, Vol. 37, No. 8, 1019–1026,

Aug. 1990.

16. Novak, I., B. Eged, and L. Hatvani, "Measurement and simulation of crosstalk reduction by discrete discontinuities along coupled PCB traces," *IEEE Transactions on Instrumentation and Measurement*, Vol. 43, No. 2, 170–175, Apr. 1994.
17. Sharma, R., T. Chakravarty, and A. B. Bhattacharyya, "Transient analysis of microstrip-like interconnections guarded by ground tracks," *Progress In Electromagnetics Research*, Vol. 82, 189–202, 2008.
18. Ladd, D. N. and G. I. Costache, "SPICE simulation used to characterize the crosstalk reduction effect of additional tracks grounded with vias on printed circuit boards," *IEEE Transactions on Circuits and Systems II: Analog and Digital Signal Processibg*, Vol. 39, No. 6, 342–347, Jun. 1992.
19. Cheng, Y. S., W. D. Guo, C. P. Hung, R. B. Wu, and D. de Zutter, "Enhanced microstrip guard trace for ringing noise suppression using a dielectric superstrate," *IEEE Transactions on Advanced Packaging*, IEEE Early Access, 2010.
20. Huang, W. T., C. H. Lu, and D. B. Lin, "Design of suppressing crosstalk by vias of serpentine guard trace," *PIERS Proceedings*, 484–488, Xian, China, Mar. 22–26, 2010.
21. Mallahzadeh, A. R., A. H. Ghasemi, S. Akhlaghi, B. Rahmati, and R. Bayderkhani, "Crosstalk reduction using step shaped transmission line," *Progress In Electromagnetics Research C*, Vol. 12, 139–148, 2010.
22. Young, B., *Digital Signal Integrity: Modeling and Simulations with Interconnects and Packages*, Prentice-Hall, 2001.
23. Lee, S. K., K. Lee, H. J. Park, and J. Y. Sim, "FEXT-eliminated stub-alternated microstrip line for multi-gigabit/second parallel links," *Electronics Letters*, Vol. 44, No. 4, 272–273, Feb. 2008.
24. Suntives, A., A. Khajooeizadeh, and R. Abhari, "Using via fences for crosstalk reduction in PCB circuits," *IEEE International Symposium on Electromagnetic Compatibility*, Vol. 1, 34–37, Aug. 2006.
25. Huang, W. T., C. H. Lu, and D. B. Lin, "The optimal number and location of grounded vias to reduce crosstalk," *Progress In Electromagnetics Research*, Vol. 95, 241–266, 2009.
26. Rodriguez-Cepeda, P., M. Ribó, F. J. Pajares, J. R. Regué, A. M. Sánchez, and A. Pérez, "Multimodal analysis of guard traces," *IEEE International Symposium on Electromagnetic Compatibility*, 1–5, Honolulu, HI, Jul. 2007.

27. Mbairi, F. D., W. P Siebert, and H. Hesselbom, "On the problem of using guard traces for high frequency differential lines crosstalk reduction," *IEEE Transactions on Components and Packaging Technologies*, Vol. 30, No. 1, 67–74, Mar. 2007.
28. IE3D User's Manual, Zeland Software, Inc, 2000.
29. Novak, I., B. Eged, and L. Hatvani, "Measurement by vector-network analyzer and simulation of crosstalk reduction on printed board with additional center traces," *IEEE Institute of Technology Conference*, 269–274, Irvine, CA, 1993.
30. Hua, R. C., C. F. Chou, S. J. Wu, and T. G. Ma, "Compact multiband planar monopole antennas for smart phone applications," *IET Microwaves, Antennas & Propagation,* Vol. 2, No. 5, 473–481, Aug. 2008.
31. Schneider, M. V., "Microstrip lines for microwave integrated circuits," *Bell System Tech. Jn.*, Vol. 48, 1422–1444, 1969.
32. Wu, T. L., Y. H. Lin, T. K. Wang, C. C. Wang, and S. T. Chen, "Electromagnetic bandgap power/ground planes for wideband suppression of ground bounce noise and radiated emission in high-speed circuits," *IEEE Transactions on Microwave Theory and Techniques*, Vol. 53, No. 9, 2935–2942, Sep. 2005.
33. Hall, S. H., G. W. Hall, and J. A. McCall, *High-speed Digital System Design: A Handbook of Interconnect Theory and Design Practices*, John-Wiley & Sons, 2000.